Wind Loads on Flush-Mounted Rooftop Solar Panels and Supporting Structural Elements

Korah Parackal, Alex Omelaniuk, David Henderson, John Ginger
Cyclone Testing Station, James Cook University, korah.parackal@jcu.edu.au

ABSTRACT
Recent damage investigations have shown that flush-mounted, rooftop solar panel arrays can be vulnerable to windstorms. This paper presents a study on the wind loads on roof-mounted solar panels using a 1/20 scale wind tunnel model. Wind pressures from a range of wind directions were recorded on the top and bottom surfaces of an instrumented panel array as well as the roof surface of a typical gable roof house. For certain approach wind directions, the presence of solar panel arrays increased the loads on the roof surface in comparison to the bare roof. Furthermore, such wind directions also produce net uplift loads on the solar panels. The larger suction pressures on the roof surface, in conjunction with the additional loads, imparted from the solar panel arrays can increase the uplift loads on batten to rafter connections. Results from this study can be used to produce design data for Codes and Standards such as AS/NZS 1170.2.

1. Introduction

Roof-mounted solar panels are increasingly common in Australia and other countries. Recent damage investigations have shown that roofs with solar panels installed can be vulnerable to wind loads (Boughton, Falck et al. 2017, Boughton, Falck et al. 2021). There is limited design data available in codes and standards for the design of the supporting structure and fastenings to the underlying roof. The Australian and New Zealand Wind Loading Standard AS/NZS 1170.2 (2021) provides net pressure coefficients for solar panels on a range of locations on inclined roofs. However, pressure coefficients on the underlying roof cladding are prescribed to be +0.6 when the net pressures on the solar panels are negative and -0.6 when the net pressures on the panels are positive.

Previous research has generally focused on determining the pressure distributions on solar panels and roofs. Leitch, Ginger et al. (2016) presented a wind tunnel model study on a 1/20-scale gable roof house. The study showed that there is the potential for uplift loads on the roof to increase when solar panels are installed on certain areas of the roof. However, due to the locations and spacing of pressure taps on the model, it was not suitable for evaluating the time-varying loads on roof structure connections. Additionally, Stenabaugh, Iida et al. (2015) presented a 1/20 scale wind tunnel study on solar panel arrays on a 30° roof pitch gable roof house. This study explored the effects of the spacing between panel arrays and the gap between the panels and the roof surface, however, it did not examine the loads on the underlying roof structure in detail.

Solar panel installations on houses in Australia generally have panels mounted parallel to inclined roofs. These panels are clamped to aluminium rails that run above the roof battens. The rails are in turn fastened to the roof battens using 'L-foot' brackets with typically one bracket per solar panel. During installation, certain roof cladding fasteners are removed and longer screws are used to fasten the L-foot brackets to the roof battens through the roof cladding.

This paper presents a wind tunnel model study on a 1/20 scale gable roof house with solar panels installed at several locations on the roof. Pressure taps on the top and bottom surface of the panels as well as on the roof surface are used to determine mean pressures on the panels and roof. Additionally, time history data from the wind tunnel study was also used to determine the uplift loads on selected batten to rafter connections considering all approach wind directions.

2. Methods

Solar panel array and roof surface loads were identified through wind tunnel model testing performed in the 2.0m high x 2.5m wide x 22m long boundary layer wind tunnel located at the James Cook University Cyclone Testing Station, shown in Figure 1. The 1/20 length scaled building and solar panel array models were attached to a turntable where 3 consecutive wind pressure test runs were sampled at 10° intervals from 0°- 360°. Wind pressures were captured on the building in the baseline case, without solar panels as well five-panel array configurations.

A building model with equivalent full-scale dimensions of 21 m in length, and 10 m in breadth with a roof pitch of 22.5° roof was chosen for the wind tunnel study. The roof structure was allocated rafter spacings of 1 m with roof battens attached to the rafters at 0.9 m spacings. A pressure tap grid consisting of 6 rows of 16 pressure taps was placed on the roof surface of the building model. Two instrumented panel array models were attached in portrait orientation (i.e., Panel widths installed parallel to the long building edge) to simulate an array of panels of 1m x 1.7m in full scale as shown in Figure 2. Each panel contained 8 pressure taps (4 top and 4 bottom) to measure pressures on the top and bottom surfaces of each panel.

Figure 1. Wind tunnel model in the boundary layer wind tunnel

Figure 2. Top view of two panels (end panel and first internal panel) in the PV array model

3. Mean Pressures

3.1 Baseline Building

The mean pressure coefficients ($C_{\bar{p},mrh}$) on the baseline building for wind directions 0°, 40°, 90°, 180°, 210°, 220° and 270° on each tap were determined and the ensemble average of the three wind tunnel runs was calculated. The $C_{\bar{p},mrh}$ values were plotted to identify the critical wind directions and the roof zones with the largest negative mean pressure coefficients. Figure 3 shows such a plot of the baseline building $C_{\bar{p},mrh}$ values for the critical wind approach direction of 210°. High suction pressures can be observed on the roof surface at the windward gable end at roof taps A1 to A6.

3.2 Configuration 4

Configuration 4 consisted of a row of 14 individual panels installed near to the ridgeline, denoted by the green outline on the roof surface of Figure 4. The critical roof surface $C_{\bar{p},mrh}$ values were found within the wind approach angle sector of 210° ± 20° in configuration 4.

The $C_{\bar{p},mrh}$ values for a wind approach angle of 210° were compared to the corresponding results of the baseline study. Little change was observed on roof surface tap rows 1 to 3 and most of the roof surface tap row 5 in comparison to the baseline case results. However, roof surface taps under the windward edges of the solar panel array were subject to higher negative pressures. Roof surface tap column B showed isolated increases in negative $C_{\bar{p},mrh}$ value by -0.5 and -1.0 from the values derived in the baseline tests at roof surface taps B5 and B4 respectively. Roof surface taps B6 to P6, nearest to the ridge line, recorded higher pressures than the baseline values with increases in negative $C_{\bar{p},mrh}$ value by -0.1 to -0.4.

Figure 3. Baseline Mean Pressure Coefficients for Wind Approach Angle 210 °

Figure 4. Configuration 4 Mean Pressure Coefficients for Wind Approach Angle 210 °

4. Time History Data Calculations

The pressures recorded in the wind tunnel study time history data files were used to identify the peak uplift forces on batten-to-rafter connections. Figure 5 illustrates the locations of two connections (R14:B5 and R2:B5) selected for analysis in this study. The batten-to-rafter connection loads were assessed by first identifying the net pressure coefficients acting on the tributary areas of the roof surface and panel array at each time step.

The largest net uplift force was then calculated using the peak pressure coefficients at the critical time step for both the roof surface and array surface. A peak design gust wind speed ($V_{des,\theta}$) of $57.5 \frac{m}{s}$ at mid-roof height was chosen for force and pressure calculations based on an average recurrence interval of 500 years within cyclonic region C in terrain category 3 as per AS/NZS 1170. (2021). This value is divided by the gust factor (G_u) to convert the velocity into an equivalent 10-minute mean wind speed for converting the mean pressure coefficients from the wind tunnel study into pressures in full scale. The peak loads acting on batten-to-rafter connections R14:B5 and R2:B5 for the baseline case

and configuration 4 were plotted against each 10° wind approach angle in Figures 6 and 7 respectively. The uplift forces on batten-to-rafter connections R14:B5 and R2:B5 are shown to be larger for close to all wind approaches compared to those recorded during the baseline tests.
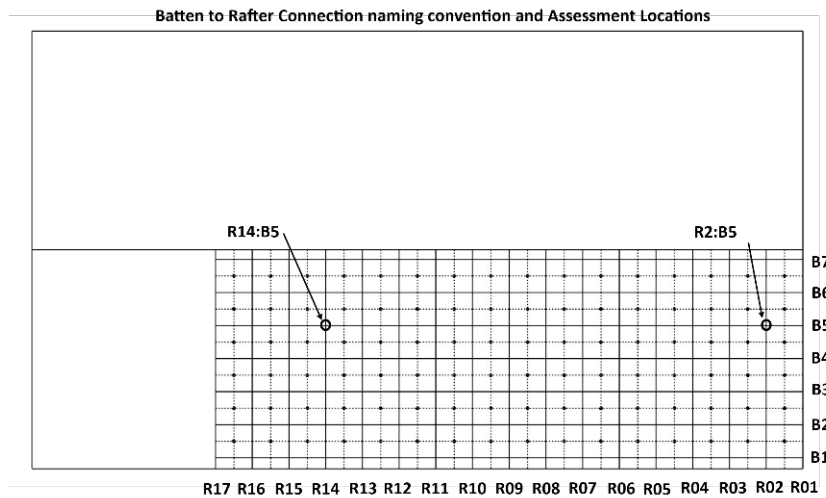

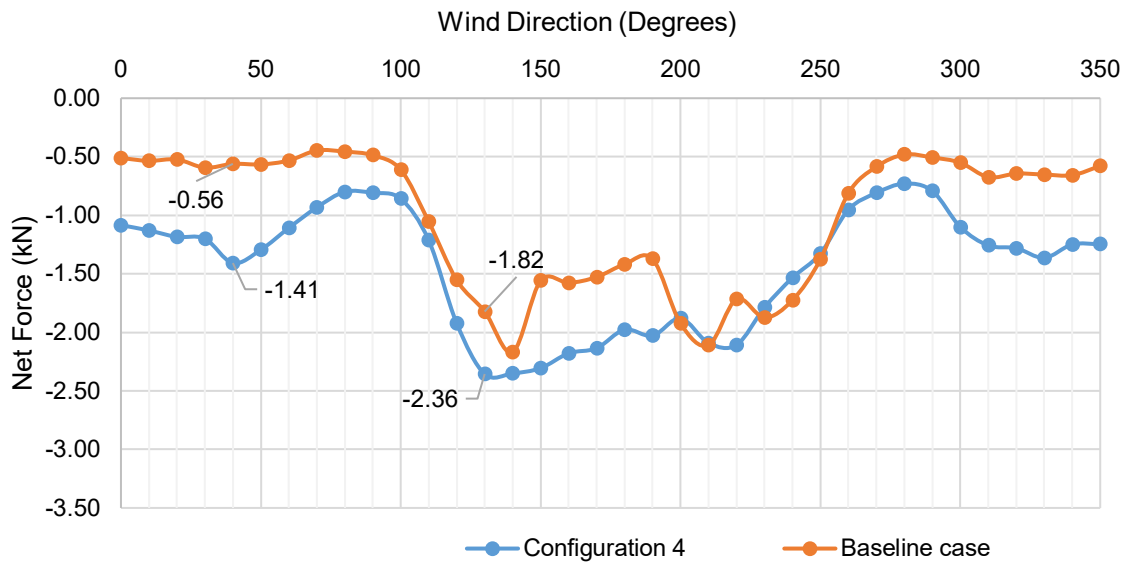Figure 5. Batten to Rafter Connection Locations and Naming Convention

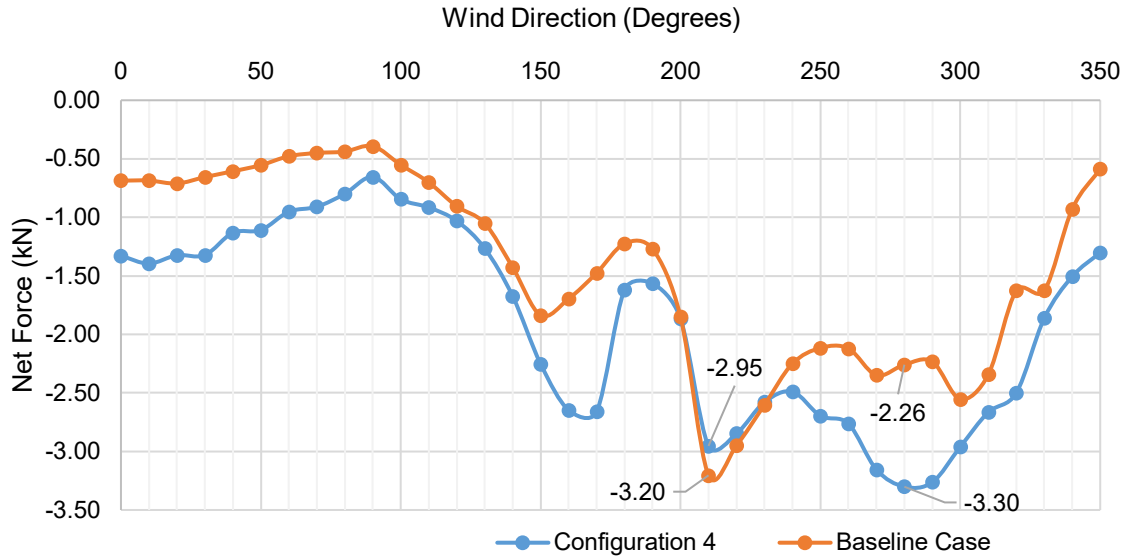Figure 6. Maximum Batten to Rafter Connection Uplift Forces on R14:B5 for all Wind Approach Angles

Wind Direction (Degrees)

Figure 7. Maximum Batten to Rafter Connection Uplift Forces on R2:B5 for all Wind Approach Angles

4. Conclusions

This study showed that roof-mounted solar panels have the potential to increase wind loads on the underlying roof structure, for certain locations of solar panels and certain batten-to-rafter connections. In most cases, net mean loads on the solar panels are close to zero due to similar wind pressures on the top and bottom surfaces acting in opposite directions. However, analysis of time history data indicates that intermitted uplift loads are experienced by the solar panels. These uplift loads, in conjunction with the additional tributary area of the solar panel, can increase the loads on batten to rafter connections. Furthermore, the data shows that peak uplift loads on solar panels do not coincide with positive pressures on the roof surface as prescribed by the Australian and New Zealand Wind Loading Standard AS/NZS 1170.2 (2021). Additional research is recommended on the effects of solar panel arrays on a range of common roof pitches and roof shapes including hip roofs.

References

Boughton, G., D. Falck, D. Henderson, D. Smith, K. Parackal, T. Kloetzke, M. Mason, R. Krupar, M. Humphreys, S. Navaratnam, G. Bodhinayake, S. Ingham and J. Ginger (2017). Tropical Cyclone Debbie: Damage to buildings in the Whitsunday Region, Cyclone Testing Station, JCU, Report TR63.

Boughton, G., D. Falck, K. Parackal, D. Henderson and G. Bodhinayake (2021). Tropical Cyclone Seroja - Damage to Buildings in the Mid-West Coastal Region of Western Australia, Cyclone Testing Station, JCU, Report TR66.

Leitch, C. J., J. D. Ginger and J. D. Holmes (2016). "Wind loads on solar panels mounted parallel to pitched roofs, and acting on the underlying roof." Wind and Structures **22**(3): 307-328.

Standards Australia (2021). AS/NZS1170.2 - Structural design actions Part 2: Wind actions. Sydney, Australia.

Stenabaugh, S. E., Y. Iida, G. A. Kopp and P. Karava (2015). "Wind loads on photovoltaic arrays mounted parallel to sloped roofs on low-rise buildings." Journal of Wind Engineering and Industrial Aerodynamics **139**: 16-26.